

# Effect of UV Exposure on IV Characteristics of a Perovskite Solar Cell

Ganga R. Neupane<sup>1,2</sup>, Susanna M. Thon<sup>2</sup>, Sheng Fu<sup>3</sup>, Zhaoning Song<sup>3</sup>, Yanfa Yan<sup>3</sup>, and Behrang H. Hamadani<sup>1</sup>

<sup>1</sup>National Institute of Standards & Technology, Gaithersburg, MD 20899, USA

<sup>2</sup>Johns Hopkins University, Baltimore, MD 21218, USA

<sup>3</sup>The University of Toledo, Toledo, OH 43606, USA

We report on the performance evolution of a perovskite solar cell under constant ultraviolet (UV) illumination measured by current-voltage scans and wide-field photoluminescence (PL) hyperspectral imaging. We observed a significant decrease in the PL intensity corresponding to a reduction in the quasi-Fermi level splitting energy after 218 hours of UV exposure. The evolving current-voltage characteristics show a constant reduction in the cell's power conversion efficiency dominated by a decrease in the fill factor, although both the open circuit voltage and the short circuit current also degrade modestly. The current-voltage measurements show a shift from a conventional hysteresis behavior to inverted hysteresis following the UV exposure of the device. The traditional double-diode model was not sufficient for accurately explaining the current density-voltage curves, so an extension to the model was necessary. The modified resistance-limited enhanced recombination model explains all the features of the current-voltage data with good accuracy. This work suggests the emergence of an additional recombination region in the cell, possibly an energetic barrier at the interface of the perovskite and the hole transport layer upon UV exposure.

## I. INTRODUCTION

Perovskite solar cells (PSCs) undergo an irreversible loss in their power conversion efficiency (PCE) due to the presence of high-energy UV photons in the solar spectrum [1]. Extensive research has been conducted to investigate the UV-induced degradation in PSCs, which contain metal-oxide electron transport layers (ETLs) such as  $\text{TiO}_2$  and  $\text{SnO}_2$ , as well as hole transport layers (HTLs) that include  $\text{NiO}$  [2], [3]. It has been reported that PSCs utilizing metal-oxide electron transport layers undergo decomposition of the absorption layer when exposed to UV light. This decomposition is attributed to the photocatalytic effect of  $\text{TiO}_2$  and  $\text{SnO}_2$  [4]. Similarly, UV irradiation on inverted PSCs with  $\text{NiO}$ -based HTLs results in the formation of voids/vacancies near the interface between the perovskite and  $\text{NiO}$  [3]. Therefore, recent work has extensively explored metal oxide alternatives as charge transport layers, such as [2-(3,6-Dimethoxy-9H-carbazol-9-yl)ethyl]phosphonic Acid (MeO-2PACz) and  $\text{C}_{60}$ /BCP (bathocuproine). However, investigations on the impact of UV exposure on PSCs containing non-metal-oxide charge transport layers are still ongoing.

In this work, we studied the effects of accelerated UV-related degradation on the electrical performance parameters and the photoluminescence (PL) response of perovskite solar cells. At several intervals during a 218-h long UV exposure, we

removed the cell to perform current density vs voltage (J-V) and hyperspectral photoluminescence imaging measurements. The J-V curves, which for the pristine cells can be easily modeled using the familiar double-diode model, deteriorated to a point that this model could no longer adequately explain the data. Severe deterioration of the fill factor (FF) initially implied an increase in the series resistance,  $R_s$ , of the device. However, the slope of the J-V curve in the forward bias regime beyond the open circuit voltage,  $V_{oc}$ , barely changes with UV degradation. Therefore, the J-V curve changes require another explanation other than changes in the shunt resistance,  $R_{sh}$ , or  $R_s$ . We were able to successfully explain the degradation data by employing the resistance-limited enhanced recombination (RLER) model [5], [6]. In this model, a third diode in series with a resistor is added to the double-diode model, possibly representing the formation of an extra energetic barrier (i.e., a local Schottky diode) in the cell. Some plausible candidates for this enhanced recombination region are a barrier formed at the HTL/perovskite interface (which directly faces the UV light on the transparent electrode side) or extra recombination losses at grain boundaries due to a systemic change within the perovskite layer itself.

The PL hyperspectral images showed a slow deterioration in the strength of the luminescence signal, pointing to an increase in the nonradiative recombination losses throughout the cell. The quasi Fermi level splitting energy, extracted from absolute PL spectra, points to a significant reduction in the internal voltage of the cell, consistent with the  $V_{oc}$  reductions observed from the J-V measurements.

## II. METHODS

### A. Solar cell device preparation

The PSCs used [7] in this study have the chemical composition  $\text{Rb}_{0.05}\text{MA}_{0.05}\text{Cs}_{0.05}\text{FA}_{0.85}\text{PbI}_{2.85}\text{Br}_{0.15}$  and the device architecture Glass/FTO/MeO-2PACz/active layer/ $\text{C}_{60}$ /BCP/Ag and were fully encapsulated during this study. Pristine cells' PCEs were typically 21 % to 22 % under the standard reporting conditions. However, the cells for this study were not fresh, and our initial PCEs prior to degradation were  $\approx 19$  %. Very little hysteresis was observed in pristine cells.

### B. Characterization approach

The cells were exposed to UV light from a 365 nm LED light source inside a black box under the normal ambient laboratory environment for a total of 218 hr. The UV light intensity was  $63 \text{ W m}^{-2}$ . The sample was periodically removed from the UV box for comprehensive characterization that included J-V curve measurements and photoluminescence hyperspectral imaging. Details about the hyperspectral measurements are reported in our previous work [8].

### III. RESULTS

Fig. 1 shows the PL photon flux emission map of a small area of the cell at 1.55 eV, showing the impact of successive UV exposure over time. All the measurements were performed at room temperature. The images reveal a gradual decrease in the luminescence of the cell after UV exposure, indicating an increase in non-radiative recombination losses across the film. Also, a larger heterogeneity occurs at the later stages. Therefore, the UV exposure does cause a degradation within the perovskite film even for encapsulated devices through a glass substrate.

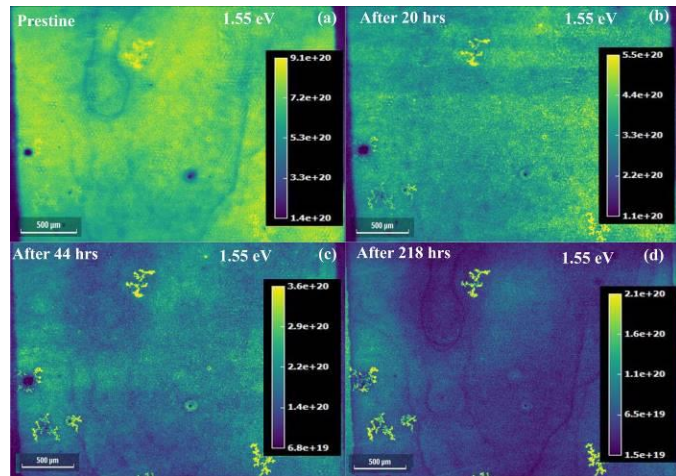


Fig. 1. PL images of a perovskite solar cell (a) with no UV exposure, (b) after 20 hrs of UV exposure, (c) after 44 hrs of UV exposure, and (d) after 218 hrs of UV exposure. The color bar represents the PL flux in photons/( $\text{m}^2 \text{ s eV}$ ) at a fixed laser intensity of  $\approx 70 \text{ mW/cm}^2$ .

Fig. 2(a) shows the absolute PL spectra corresponding to each UV exposure time. The emission spectra consist of a broad single peak centered at approximately 1.55 eV, corresponding to the band-to-band transition of the perovskite layer. While the peak position remains constant, there is a gradual reduction in peak intensity. From the absolute PL photon flux, the quasi Fermi level splitting energy,  $\Delta\mu$ , which corresponds to the internal voltage,  $iV$  ( $\Delta\mu = q iV$ ) can be estimated under this excitation source, with  $q$  as the elementary charge. The spontaneous radiative emission in terms of the spectral absorptivity under non-equilibrium condition is given by [9]:

$$I_{PL}(E) = \frac{2\pi}{c^2 h^3} \frac{E^2 a(E)}{\exp((E - \Delta\mu)/kT) - 1} \quad (1)$$

where  $I_{PL}$  is the spectral PL photon flux as a function of energy  $E$ ,  $h$  is the Planck constant,  $a$  is the absorptivity,  $k$  is the Boltzmann constant,  $c$  is the speed of light, and  $T$  is the temperature. The key assumption made in estimating the  $\Delta\mu$  value is that the absorption for energies in the high energy regime is unity. The extracted  $\Delta\mu$  values are shown in Fig. 2(b) and show a substantial reduction in the  $iV$  of the device with UV exposure. Indeed, this observation is consistent with the  $V_{oc}$  reductions shown next and points to an increase in the formation of nonradiative recombination centers.

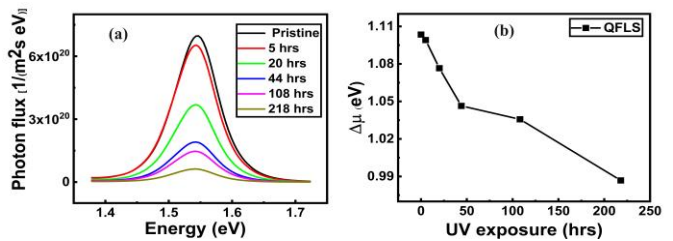


Fig. 2. (a) Spectral PL photon flux under different UV exposure times and (b) the quasi-Fermi level splitting energy with increasing UV exposure.

Next, we discuss the J-V changes upon each successive UV exposure. Fig. 3(a) shows the forward and reverse direction J-V curve sweeps after each exposure interval. As exposure time increases, we observe a clear degradation trend in all J-V curve parameters, as shown in Table 1. However, the largest change occurs with the FF of the device, dropping precipitously to near 50 %. The small hysteresis observed in the initial stages of the monitoring is typical with these devices, with the reverse sweep showing slightly more favorable device parameters.

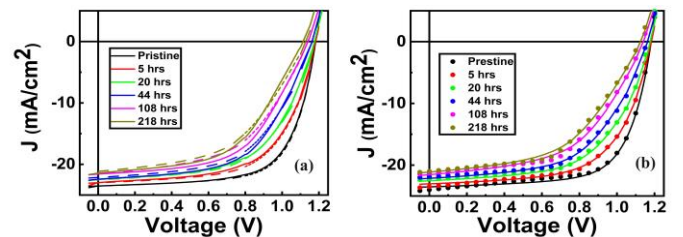


Fig. 3. (a) J-V characteristics of a PSC at different UV exposure times with forward (solid line) and reverse (dashed) scans, and (b) J-V characteristics of the PSC fitted with the RLRL model. The symbols represent the model calculations whereas the solid lines are the experimental data. For the sake of simplicity, the data presented in (b), both experimental and model, are from the reverse sweep direction.

Table. 1. Parameters extracted from the J-V measurements.

	Bias	Voc (V)	Jsc ( $\text{mA/cm}^2$ )	FF (%)	PCE (%)
Pristine	Forward	1.18	23.54	66.88	18.62
	Reverse	1.18	23.53	67.73	18.85
5 hrs	Forward	1.18	22.97	61.13	16.61

		Reverse	1.18	23.03	61.58	16.79
20 hrs	Forward	1.17	22.49	58.20	15.39	
	Reverse	1.18	22.53	57.79	15.38	
	Forward	1.16	22.42	56.85	14.82	
44 hrs	Reverse	1.16	22.14	55.54	14.31	
	Forward	1.14	21.58	55.31	13.61	
	Reverse	1.14	21.54	52.43	12.89	
108 hrs	Forward	1.12	21.39	53.05	12.64	
	Reverse	1.13	21.13	50.81	12.14	

However, this conventional hysteresis pattern, observed in the pristine cell, undergoes a noticeable transformation to inverted hysteresis as UV exposure progresses, causing the forward sweep direction to become more favorable near the end of the exposure period. This inverted hysteresis behavior has been attributed to the formation of an energy barrier at the interface of perovskite and charge transport layers [10]. We believe that the constant UV exposure induces a barrier at the perovskite/HTL interface, causing additional recombination losses, specifically near the knee of the J-V curve.

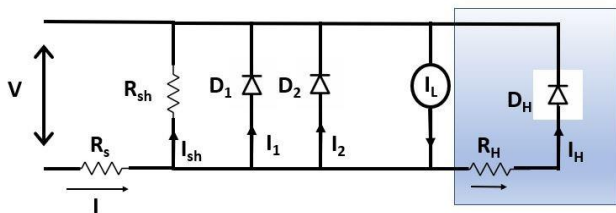


Fig. 4. Equivalent circuit of the resistance-limited enhanced recombination model.

To investigate the effect of this barrier formation with UV exposure, we used the RLER model, which is similar to a double-diode model with an additional diode element denoted as  $D_H$ , in series with a resistance element  $R_H$ , as shown in Fig. 4. We solved and fit this model numerically to our experimental light J-V curves, as shown in Fig. 3(b). The saturation current densities,  $J_{01}$  (for  $D_1$ ) and  $J_{02}$  (for  $D_2$ ), and shunt resistance ( $R_{sh}$ ) were determined to be  $6.4 \times 10^{-20} \text{ mA/cm}^2$ ,  $4.13 \times 10^{-10} \text{ mA/cm}^2$ , and  $367.20 \Omega \text{ cm}^2$ , respectively, and were found to remain constant across all consecutive measurements. The changing parameters extracted from the model are presented in Table 2.

Table. 2. Extracted parameters from the resistance-limited enhanced recombination model.

	0 hrs	5 hrs	20 hrs	44 hrs	108 hrs	218 hrs
$J_L (\text{mA/cm}^2)$	21.66	21.20	20.74	20.18	19.35	19.07
$R_s (\Omega \text{cm}^2)$	4.01	4.01	5.29	6.21	6.26	6.53
$J_{0H}$ ( $\text{mA/cm}^2$ )	$1.93 \times 10^{-17}$	$7.35 \times 10^{-16}$	$2.46 \times 10^{-15}$	$7.59 \times 10^{-15}$	$1.80 \times 10^{-14}$	$5.51 \times 10^{-14}$
$R_H (\Omega \text{cm}^2)$	32.72	32.29	29.81	26.46	21.06	20.41

Here, the parameters  $J_L$  and  $J_{0H}$  are the photo-induced current density and the reverse saturation current density for  $D_H$ , respectively. Examining the fit parameters, it is evident that

there is a gradual increase in  $J_{0H}$ , reaching up to  $5.51 \times 10^{-14} \text{ mA/cm}^2$ , a three orders of magnitude change, after 218 hours of UV exposure. This increase in  $J_{0H}$  suggests an increase in non-radiative recombination within the cell stack. This finding agrees well with our earlier observation of a decrease in PL intensity and the  $\Delta\mu$  trend from PL imaging. We believe that as the cell ages, the aforementioned energy barrier becomes larger, hence causing larger current losses across it. Recombination losses at this junction would result in less PL emission from the film, but the fact that the PL response is heterogeneous suggests that the barrier formation is not uniform across the whole of the device area but rather can be patchy and regional.

#### IV. SUMMARY

In this study, we systematically aged a perovskite solar cell under UV radiation and investigated the J-V characteristics and PL response during this process. The J-V curves can be successfully explained with a resistance-limited enhanced recombination model that incorporates an extra recombination region within the cell. It is highly likely that this recombination region is the result of an energetic barrier formation either at the HTL/perovskite interface or at grain boundaries. The PL measurements validate the J-V curve changes, particularly the degradation observed in the  $V_{oc}$ . Additional characterization methods, such as transient techniques, could yield additional information on the nature of changes observed in these cells.

#### REFERENCES

- [1] A. Valluvar Oli, Z. Li, Y. Chen, and A. Ivaturi, "Near-Ultraviolet Indoor Black Light-Harvesting Perovskite Solar Cells," *ACS Appl Energy Mater*, vol. 5, no. 12, pp. 14669–14679, Dec. 2022, doi: 10.1021/acsaelm.2c01560.
- [2] J. Ji *et al.*, "Two-Stage Ultraviolet Degradation of Perovskite Solar Cells Induced by the Oxygen Vacancy-Ti4+ States," *iScience*, vol. 23, no. 4, p. 101013, 2020, doi: 10.1016/j.isci.2020.101013.
- [3] X. Zhu *et al.*, "Inverted planar heterojunction perovskite solar cells with high ultraviolet stability," *Nano Energy*, vol. 103, no. PB, p. 107849, Dec. 2022, doi: 10.1016/j.nanoen.2022.107849.
- [4] T. Chen, J. Xie, and P. Gao, "Ultraviolet Photocatalytic Degradation of Perovskite Solar Cells: Progress, Challenges, and Strategies," *Advanced Energy and Sustainability Research*, vol. 3, no. 6, Jun. 2022, doi: 10.1002/aesr.202100218.
- [5] K. R. McIntosh, "Lumps, Humps and Bumps: Three Detrimental Effects in the Current-Voltage Curve of Silicon Solar Cells," 2001. doi: 10.13140/RG.2.2.19197.26083.
- [6] F. Hernando, R. Gutierrez, G. Bueno, F. Recart, and V. Rodriguez, "Humps, a surface damage explanation," *Proceedings of the 2nd World Conference on Photovoltaic Solar Energy Conversion*, vol. 6–10, no. July, pp. 1321–1323, 1998.
- [7] Q. Jiang *et al.*, "Surface reaction for efficient and stable inverted perovskite solar cells," *Nature*, vol. 611, no. 7935, pp. 278–283, Nov. 2022, doi: 10.1038/s41586-022-05268-x.
- [8] G. R. Neupane *et al.*, "Imaging local luminescence variations in CdSe0.1Te0.9 thin films grown by the colossal grain growth process," *Cell Rep Phys Sci*, vol. 4, no. 8, p. 101522, 2023, doi: 10.1016/j.xrpp.2023.101522.
- [9] J. K. Katahara and H. W. Hillhouse, "Quasi-Fermi level splitting and sub-bandgap absorptivity from semiconductor photoluminescence," *J Appl Phys*, vol. 116, no. 17, Nov. 2014, doi: 10.1063/1.4898346.
- [10] F. Wu *et al.*, "Inverted Current–Voltage Hysteresis in Perovskite Solar Cells," *ACS Energy Lett*, vol. 3, no. 10, pp. 2457–2460, Oct. 2018, doi: 10.1021/acsenergylett.8b0

